Contemporary Mathematics
https://ojs.wiserpub.com/index.php/CM/

Research Article

A Spectral Collocation Approach for Time-Fractional Korteweg-de Vries-Burgers Equation via First-Kind Chebyshev Polynomials

Y. H. Youssri[1,2], Laila A. Alnaser[3*], A. G. Atta[4]

[1] Department of Mathematics, Faculty of Science, Cairo University, Giza, 12613, Egypt
[2] Faculty of Engineering, Egypt University of Informatics, Knowledge City, New Administrative Capital, 19519, Egypt
[3] Department of Mathematics, College of Science, Taibah University, Al Madina Al Munawara, 41411, Kingdom of Saudi Arabia
[4] Department of Mathematics, Faculty of Education, Ain Shams University, Roxy, 11341, Cairo, Egypt
E-mail: lnaser@taibahu.edu.sa

Received: 21 October 2024; **Revised:** 6 February 2025; **Accepted:** 10 February 2025

Abstract: The time-fractional Korteweg-de Vries-Burgers (TFKdVB) problem is solved numerically in this study. The approach makes use of the shifted first-kind Chebyshev polynomials (SFKCPs) collocation method. By utilizing Caputo's formulation to approximate the time-fractional derivatives and impose boundary conditions, we arrive at a spectral solution. Numerical examples are presented to illustrate the precision and effectiveness of the suggested approach.

***Keywords*:** first kind chebyshev polynomials, collocation method, time-fractional KdV-Burgers' equation

MSC: 35R11, 65M70, 35Q53, 41A10, 65N35

1. Introduction

Korteweg and De Vries [1] developed the Korteweg-de Vries (KdV) equation in 1895 to improve understanding of the dynamics of weakly nonlinear waves. Since its origin, this equation has been a basic tool for studying a wide range of physical phenomena in various disciplines. Su and Gardner [2] developed the (KdVB) equation, which is particularly useful for investigating the interplay of dispersion, dissipation, and nonlinearity in wave propagation through an elastic conduit filled with fluid. Furthermore, the fractional TFKdVB equation [3], the fractional Schrödinger-Korteweg-de Vries equation [4], and the fractional Burgers' equation [5] are modern nonlinear fractional partial differential equations proposed to explain critical phenomena and intricate dynamic processes in the realm of physics. The KdVB equation is a fundamental tool used to describe many scientific processes, including wave propagation, traffic flow models, and fluid dynamics. An extension of the classical form, which includes a fractional derivative with respect to time [6–8], is the TFKdVB equation, enabling the representation of anomalous diffusion and non-local behavior. Fractional derivatives provide a more accurate depiction of some physical systems because they reflect the memory and heredity features of the related processes. Because of this, the TFKdVB equation is an essential tool for comprehending complex dynamics that are inexpressible in standard integer-order models [9–11].

There are several real-world applications for the TFKdVB equation. It can simulate fluid flow in pipes, for instance, where memory effects affect the flow. It is especially helpful in explaining how waves behave in materials like elastic

DOI: https://doi.org/10.37256/cm.6220255948

solids, where material characteristics and time-dependent effects are significant. This equation is useful in environmental research since it may also be used to predict the dispersion of pollutants in rivers or oceans, where the dispersion is influenced by historical conditions. Technically speaking, time-fractional equations have garnered the attention of many researchers due to their wide range of applications. Several methods for treating time-fractional equations have been developed, including the Fractional Non-Polynomial Spline Method, the Homotopy Perturbation Method, the Hyperbolic Non-Polynomial Spline Approach, and the Ansatz Method [12–14].

Chebyshev polynomials, a family of orthogonal polynomials, have proven to be highly effective in numerical analysis, particularly for solving differential equations. Their strong approximation properties make them well-suited for spectral methods. When high accuracy is needed, their recursive relations and orthogonality simplify complex problems. Chebyshev polynomials make it easier to describe solutions in series form when solving fractional differential equations, offering a productive method for approximating solutions over a predetermined interval [15–18].

The spectral collocation method is an exceptionally accurate numerical technique for solving differential equations, especially those involving fractional derivatives. It works by discretizing the domain into collocation points, where the solution must exactly satisfy the equation, transforming the differential equation into a system of algebraic equations. This strategy works especially well because it combines the ease of use of collocation techniques with the quick convergence of spectral methods. The spectral collocation method becomes an effective tool for solving fractional differential equations that are both linear and nonlinear when combined with Chebyshev polynomials [19, 20].

The application of spectral methods to fractional differential equation solving has been investigated in a number of publications. Due of their precision and efficiency, spectral approaches such as Petrov-Galerkin, Galerkin, and collocation methods have been used to fractional models in recent years. Research has demonstrated that spectral methods, especially when combined with orthogonal polynomials like Chebyshev or Legendre polynomials, can yield high-precision results even with fewer collocation points. Furthermore, numerous researchers have applied these methods to time-fractional equations, showing their potential in modeling physical systems with memory and hereditary properties [21–27].

Recent work in numerical methods for fractional problems have highlighted the need for robust and effective methods to tackle the difficulties these equations present. Because of its nonlinearity and presence of fractional derivatives, TFKdVB equation is especially difficult. In response, scientists have investigated a number of numerical techniques, including as spectral, finite difference, and finite element methods, to provide very accurate approximations of solutions. Spectral approaches are notable for their exceptional convergence characteristics and computational effectiveness, especially when paired with orthogonal polynomials such as Chebyshev or Legendre polynomials. By presenting a collection of SFKCPs designed to precisely and effectively solve the TFKdVB problem, this work expands on prior developments. In this study, we provide a Chebyshev polynomial-based TFKdVB equation solution method for spectral collocation. The spatial domain is then discretized using the spectral collocation method, and the resulting system of equations is solved. Numerous numerical examples that show the convergence of the suggested method are used to validate the accuracy of the approach. Our findings demonstrate that, even with a comparatively limited number of collocation points, the spectral collocation method offers a reliable and efficient solution for the TFKdVB equation.

The suggested the approach presents a novel use of modified sets of SFKCPs in collocation method, providing an accurate, efficient and fast numerical scheme for spectrally solving the TFKdVB. It addresses important difficulties in computational complexity and stability, employing few computer resources and greatly improving solution accuracy when compared to existing approaches. To the best of our knowledge, the main contribution and novelty of this paper can be listed in the following points:

• A new theoretical background to the SFKCPs are presented.

• Deriving new theorems of integer and fractional derivatives for the modified sets of SFKCPs. These theorems are considered important tools for treating TFKdVB.

The advantages of the presented approach are as follows.

• By choosing modified sets of SFKCPs as basis functions, some terms of the retained modes make it produce approximations with promising precision.

• Fewer calculations are required to obtain the approximate solution desired.

2. Preliminaries and fundamental formulae

2.1 *The caputo sense of the fractional derivative*

Definition 1 [28] The definition of the Caputo fractional derivative of order s is:

$$D_{\rho}^{m}\zeta(\rho)=\frac{1}{\Gamma(m-s)}\int_{0}^{\rho}(\rho-n)^{m-s-1}\zeta^{(m)}(n)dn,\quad s>0,\quad \rho>0, \tag{1}$$

where $s\in(m-1,\,m]$, $m\in\mathbb{N}$.

The operator D_{ρ}^{s} for $s\in(m-1,\,m]$, $m\in\mathbb{N}$, satisfies the following characteristics.

$$D_{\rho}^{s}c=0,\ \ (c \text{ is a constant}) \tag{2}$$

$$D_{\rho}^{s}\rho^{m}=\begin{cases}0, & \text{if } m\in\mathbb{N}_0 \quad \text{and} \quad m<\lceil s\rceil,\\ \dfrac{(m)!}{\Gamma(m-s+1)}\rho^{m-s}, & \text{if } m\in\mathbb{N}_0 \quad \text{and} \quad m\geq\lceil s\rceil,\end{cases} \tag{3}$$

where $\mathbb{N}=\{1,\,2,\,3,\,...\}$, $\mathbb{N}_0=\{0\}\cup\mathbb{N}$ and the notation $\lceil\alpha\rceil$ denotes the ceiling function.

2.2 *Few properties of the shifted Chebyshev polynomials*

The SFKCPs $T_j^*(\rho)$ is defined in the interval $[0,\,1]$ by $T_r^*(\rho)=T_r(2\rho-1)$, these polynomials can be defined as [29]:

$$T_r^*(\rho)=r\sum_{k=0}^{r}\frac{(-1)^{r-k}2^{2k}(r+k-1)!}{(r-k)!\,(2k)!}\rho^{k},\quad r>0, \tag{4}$$

and fulfilling the following orthogonality relation [29]:

$$\int_{0}^{1}\hat{w}(\rho)\,T_r^*(\rho)\,T_q^*(\rho)\,dx=h_r\,\delta_{r,\,q}, \tag{5}$$

where $\hat{w}(\rho)=\dfrac{1}{\sqrt{\rho\,(1-\rho)}}$,

$$h_r=\begin{cases}\pi, & \text{if } r=0,\\ \dfrac{\pi}{2}, & \text{if } r>0,\end{cases} \tag{6}$$

and

$$\delta_{r,\,q} = \begin{cases} 1, & \text{if } r = q, \\ \\ 0, & \text{if } r \neq q. \end{cases} \tag{7}$$

The recurrence relation of $T_r^*(\rho)$ is

$$T_{r+1}^*(\rho) = 2\,(2\rho - 1)\,T_r^*(\rho) - T_{r-1}^*(\rho), \tag{8}$$

where $T_0^*(\rho) = 1$, $T_1^*(\rho) = 2\rho - 1$.

Moreover, the inversion formula is [29]

$$\rho^r = 2^{1-2r}\,(2r)!\,\sum_{p=0}^{r} \frac{\varepsilon_p}{(r-p)!(r+p)!}\,T_p^*(\rho), \quad r \geq 0, \tag{9}$$

where

$$\varepsilon_m = \begin{cases} \dfrac{1}{2}, & \text{if } m = 0, \\ \\ 1, & \text{otherwise.} \end{cases} \tag{10}$$

Corollary 1 [30] The qth derivative of $T_j^*(\rho)$ for each positive integer q can be written as:

$$D^q\,T_j^*(\rho) = \sum_{\substack{p=0 \\ (j+p+q)\ even}}^{j-q} d_{j,\,p,\,q}\,T_p^*(\rho), \tag{11}$$

where

$$d_{j,\,p,\,q} = \frac{j\,2^{2q}\,\varepsilon_p\,(q)_{\frac{1}{2}(j-p-q)}}{\left(\dfrac{1}{2}(j-p-q)\right)!\left(\dfrac{1}{2}(j+p+q)\right)_{1-q}}, \tag{12}$$

and ε_p defined in (10).

Lemma 1 [31] For $m,\ n \in \mathbb{N}_0$, the following linearization formula holds for $T_m^*(\rho)$

$$T_m^*(\rho)\,T_n^*(\rho) = \frac{1}{2}\left(T_{m+n}^*(\rho) + T_{|m-n|}^*(\rho)\right) \tag{13}$$

Corollary 2 The following derivatives of $T_i^*(\rho)$ hold

$$\frac{d\,T_i^*(\rho)}{d\,\rho} = \sum_{p=0}^{i-1} \mathscr{A}_{p,i}\, T_p^*(\rho), \quad i \geq 1, \tag{14}$$

$$\frac{d^2\,T_i^*(\rho)}{d\,\rho^2} = \sum_{p=0}^{i-2} \mathscr{B}_{p,i}\, T_p^*(\rho), \quad i \geq 2, \tag{15}$$

$$\frac{d^3\,T_i^*(\rho)}{d\,\rho^3} = \sum_{p=0}^{i-3} \mathscr{C}_{p,i}\, T_p^*(\rho), \quad i \geq 3, \tag{16}$$

where

$$\mathscr{A}_{p,i} = 2\,i \begin{cases} 1, & (p+i+1) \text{ even}, \ p=0, \\ 2, & (p+i+1) \text{ even}, \\ 0, & \text{otherwise}, \end{cases} \tag{17}$$

$$\mathscr{B}_{p,i} = 2\,i\,(i-p)\,(i+p) \begin{cases} 1, & (p+i+2) \text{ even}, \ p=0, \\ 2, & (p+i+2) \text{ even}, \\ 0, & \text{otherwise}, \end{cases} \tag{18}$$

$$\mathscr{C}_{p,i} = i\,(i-p-1)\,(i-p+1)\,(i+p-1)\,(i+p+1) \begin{cases} 1, & (p+i+3) \text{ even}, \ p=0, \\ 2, & (p+i+3) \text{ even}, \\ 0, & \text{otherwise}. \end{cases} \tag{19}$$

Proof. The proof of Corollary 2 can be directly obtained after taking $q = 1, 2, 3$ respectively and simplifying the result in Theorem 1. □

3. Collocation technique for TFKdVB equation

In this section, we consider the following TFKdVB equation [32]

$$D_t^{\alpha}\varphi(\rho,t) + k\,\varphi(\rho,t)\,\varphi_{\rho}(\rho,t) - \upsilon\,\varphi_{\rho\rho}(\rho,t) + \mu\,\varphi_{\rho\rho\rho}(\rho,t) = s(\rho,t), \quad \alpha \in (0,1), \tag{20}$$

subject to the following initial condition

$$\varphi(\rho, 0) = a_0(\rho), \quad \rho \in [0, 1], \tag{21}$$

and boundary conditions

$$\varphi(0, t) = a_1(t), \ \ \varphi(1, t) = a_2(t), \ \ \varphi_\rho(1, t) = a_2(t), \quad t \in [0, 1], \tag{22}$$

where $s(\rho, t)$ is the source term and $k \neq 0, \ \upsilon, \mu$ are positive parameters.

3.1 *Trial functions*

Assuming the following basis functions

$$\begin{aligned} \mathscr{X}_i(\rho) &= T_i^*(\rho) - \frac{i+1}{i+2} T_{i+1}^*(\rho) - T_{i+2}^*(\rho) + \frac{i+1}{i+2} T_{i+3}^*(\rho), \\ \mathscr{T}_j(t) &= t^\alpha T_j^*(t). \end{aligned} \tag{23}$$

Remark 1 The basis functions defined in (23) satisfy the following conditions

$$\mathscr{X}_i(0) = \mathscr{X}_i(1) = \mathscr{X}_i'(1) = \mathscr{T}_j(0) = 0. \tag{24}$$

Lemma 2 The following three derivatives of $\mathscr{X}_i(\rho)$ can be expressed explicitly as:

$$\begin{aligned} \frac{d\,\mathscr{X}_i(\rho)}{d\rho} &= \sum_{p=0}^{i-1} \mathscr{A}_{p,i} T_p^*(\rho) - \frac{i+1}{i+2} \sum_{p=0}^{i} \mathscr{A}_{p,i+1} T_p^*(\rho) - \sum_{p=0}^{i+1} \mathscr{A}_{p,i+2} T_p^*(\rho) + \frac{i+1}{i+2} \sum_{p=0}^{i+2} \mathscr{A}_{p,i+3} T_p^*(\rho), \\ \frac{d^2\,\mathscr{X}_i(\rho)}{d\rho^2} &= \sum_{p=0}^{i-2} \mathscr{B}_{p,i} T_p^*(\rho) - \frac{i+1}{i+2} \sum_{p=0}^{i-1} \mathscr{B}_{p,i+1} T_p^*(\rho) - \sum_{p=0}^{i} \mathscr{B}_{p,i+2} T_p^*(\rho) + \frac{i+1}{i+2} \sum_{p=0}^{i+1} \mathscr{B}_{p,i+3} T_p^*(\rho), \\ \frac{d^3\,\mathscr{X}_i(\rho)}{d\rho^3} &= \sum_{p=0}^{i-3} \mathscr{C}_{p,i} T_p^*(\rho) - \frac{i+1}{i+2} \sum_{p=0}^{i-2} \mathscr{C}_{p,i+1} T_p^*(\rho) - \sum_{p=0}^{i-1} \mathscr{C}_{p,i+2} T_p^*(\rho) + \frac{i+1}{i+2} \sum_{p=0}^{i} \mathscr{C}_{p,i+3} T_p^*(\rho). \end{aligned} \tag{25}$$

Proof. The proof of this Lemma can be obtained after using Corollary 2 along with the definition of $\mathscr{X}_i(\rho)$ in (23). □

Theorem 1 The following fractional derivative of order $\alpha \in [0, 1]$ for $\mathscr{T}_j(t)$ is

$$D_t^\alpha \mathscr{T}_j(t) = \sum_{k=1}^{j} \mathscr{F}_{k,j} T_k^*(t) + \mathscr{G}_j, \tag{26}$$

where

$$\mathscr{F}_{k,\,j}=\frac{2j(-1)^{j-k}\Gamma\left(k+\frac{3}{2}\right)\Gamma(k+j)}{\Gamma(j-k+1)}\,{}_3\tilde{F}_2\left(\begin{array}{c|c} k+\frac{3}{2},\,k-j,\,k+j & \\ & 1 \\ k+1,\,2k+1 & \end{array}\right), \tag{27}$$

and

$$\mathscr{G}_j=\frac{1}{2}\sqrt{\pi}(-1)^j\,{}_3\tilde{F}_2\left(\begin{array}{c|c} \frac{3}{2},\,-j,\,j & \\ & 1 \\ 1,\,1 & \end{array}\right). \tag{28}$$

Proof. Using the connection (4), the power form of $\mathscr{T}_j(t)$ may be expressed as

$$D_t^{\alpha}\mathscr{T}_j(t)=\sum_{k=0}^{j}\frac{j2^{2k}(-1)^{j-k}(k+j-1)!\Gamma(\alpha+k+1)}{(2k)!\,(j-k)!\,k!}\,t^k. \tag{29}$$

The inversion formula (9) can be used to rewrite the last equation as

$$D_t^{\alpha}\mathscr{T}_j(t)=\sum_{k=0}^{j}\frac{j2^{2k}(-1)^{j-k}(k+j-1)!\Gamma(\alpha+k+1)}{(2k)!\,(j-k)!\,k!}\left(\frac{4^{-k}(2k)!}{(k!)^2}+\sum_{p=1}^{k}\frac{2^{1-2k}(2k)!}{(k-p)!\,(k+p)!}\,T_p^*(t)\right). \tag{30}$$

Once the terms in the previous equation have been expanded and rearranged, one has

$$D_t^{\alpha}\mathscr{T}_j(t)=\sum_{k=1}^{j}\sum_{p=k}^{j}\frac{2j(-1)^{j-p}\Gamma(j+p)\Gamma(p+\alpha+1)}{p!(j-p)!(p-k)!(k+p)!}\,T_k^*(t)+\sum_{k=0}^{j}\frac{j(-1)^{j-k}\Gamma(k+j)\Gamma(k+\alpha+1)}{(k!)^3(j-k)!}, \tag{31}$$

The following simplified forms can now be obtained by summed the following summations

$$\mathscr{G}_j=\sum_{k=0}^{j}\frac{j(-1)^{j-k}\Gamma(k+j)\Gamma(k+\alpha+1)}{(k!)^3(j-k)!}=\frac{1}{2}\sqrt{\pi}(-1)^j\,{}_3\tilde{F}_2\left(\begin{array}{c|c} \frac{3}{2},\,-j,\,j & \\ & 1 \\ 1,\,1 & \end{array}\right), \tag{32}$$

and

$$\mathscr{F}_{k,\,j} = \sum_{p=k}^{j} \frac{2j(-1)^{j-p}\Gamma(j+p)\Gamma(p+\alpha+1)}{p!(j-p)!(p-k)!(k+p)!}$$

$$= \frac{2j(-1)^{j-k}\Gamma\left(k+\frac{3}{2}\right)\Gamma(k+j)}{\Gamma(j-k+1)}\,{}_3\tilde{F}_2\left(\begin{matrix} k+\frac{3}{2},\, k-j,\, k+j \\ k+1,\, 2k+1 \end{matrix}\,\middle|\, 1\right). \tag{33}$$

Therefore, we get the following relation

$$D_t^{\alpha}\mathscr{T}_j(t) = \sum_{k=1}^{j} \mathscr{F}_{k,\,j}\,T_k^*(t) + \mathscr{G}_j. \tag{34}$$

This completes the proof of Theorem 1. □

3.2 *Collocation solution for the TFKdVB equation*

We will apply the following transformation in order to move on with our suggested collocation strategy:

$$\zeta(\rho, t) = \varphi(\rho, t) + g(\rho, t), \tag{35}$$

where

$$g(\rho, t) = \rho\,(\rho-1)\,\left(\varphi_\rho(1,0) - \varphi_\rho(1,t)\right) - (\rho-1)^2\,\varphi(0,t)$$
$$+ (\rho-2)\,\rho\,\varphi(1,t) + (\rho-1)^2\,\varphi(0,0) - (\rho-2)\,\rho\,\varphi(1,0) - \varphi(\rho,0), \tag{36}$$

Now, the TFKdVB equation (20), which is regulated by the criteria (21) and (22), was transformed into the following modified equation using (35):

$$D_t^{\alpha}\zeta(\rho,t) + k\,\zeta(\rho,t)\,\zeta_\rho(\rho,t) - \upsilon\,\zeta_{\rho\rho}(\rho,t) + \mu\,\zeta_{\rho\rho\rho}(\rho,t) - k\,\zeta(\rho,t)\,g_\rho(\rho,t)$$
$$- k\,\zeta_\rho(\rho,t)\,g(\rho,t) = f(\rho,t),\ \alpha \in (0,1), \tag{37}$$

with the homogeneous conditions

$$\zeta(\rho,0) = 0,\ \ \rho \in [0,1], \tag{38}$$

$$\zeta(0,t) = \zeta(1,t) = \zeta_\rho(1,t) = 0,\ \ t \in [0,1], \tag{39}$$

where

$$f(\rho,t)=s(\rho,t)+D_t^{\alpha}g(\rho,t)-k\,g(\rho,t)\,g_{\rho}(\rho,t)-\upsilon\,g_{\rho\rho}(\rho,t)+\mu\,g_{\rho\rho\rho}(\rho,t). \tag{40}$$

Consequently, we can solve the modified equation (37) guided by the homogeneous conditions (38) and (39) rather than (20) governed by (21) and (22).

Now, one may set

$$\begin{aligned}&\mathscr{L}^{M}=\text{span}\{\mathscr{X}_i(\rho)\,\mathscr{T}_j(t):i,\ j=0,\,1,\,\ldots,\,M\},\\&\mathscr{N}^{M}=\{\zeta\in\mathscr{L}^{M}:\zeta(\rho,0)=\zeta(0,t)=\zeta(1,t)=\zeta_{\rho}(1,t)=0\},\end{aligned} \tag{41}$$

then, any function $\zeta^{M}(\rho,t)\in\mathscr{N}^{M}$ may be expressed as

$$\zeta^{M}(\rho,t)=\sum_{i=0}^{M}\sum_{j=0}^{M}\hat{\zeta}_{ij}\,\mathscr{X}_i(\rho)\,\mathscr{T}_j(t). \tag{42}$$

The residual $\mathbb{RES}(\rho,t)$ of equation (37) can be written as

$$\begin{aligned}\mathbb{RES}(\rho,t)=&D_t^{\alpha}\zeta^{M}(\rho,t)+k\,\zeta^{M}(\rho,t)\,\zeta_{\rho}^{M}(\rho,t)-\upsilon\,\zeta_{\rho\rho}^{M}(\rho,t)+\mu\,\zeta_{\rho\rho\rho}^{M}(\rho,t)\\&-k\,\zeta^{M}(\rho,t)\,g_{\rho}(\rho,t)-k\,\zeta_{\rho}^{M}(\rho,t)\,g(\rho,t)-f(\rho,t)\end{aligned} \tag{43}$$

Now, we're going to get the expressions of $D_t^{\alpha}\zeta^{M}(\rho,t)$, $\zeta^{M}(\rho,t)\,\zeta_{\rho}^{M}(\rho,t)$, $\zeta_{\rho\rho}^{M}(\rho,t)$ and $\zeta_{\rho\rho\rho}^{M}(\rho,t)$.
By virtue of Theorem 1, Lemma 2 and the definition of basis functions defined in (23), one has

$$\begin{aligned}&D_t^{\alpha}\zeta^{M}(\rho,t)\\&=\sum_{i=0}^{M}\sum_{j=0}^{M}\hat{\zeta}_{ij}\,\mathscr{X}_i(\rho)\left(\sum_{k=1}^{j}\left(\mathscr{F}_{k,\,j}\,T_k^{*}(t)+\mathscr{G}_j\right)\right)\\&=\sum_{i=0}^{M}\sum_{j=0}^{M}\hat{\zeta}_{ij}\left(T_i^{*}(\rho)-\frac{i+1}{i+2}\,T_{i+1}^{*}(\rho)-T_{i+2}^{*}(\rho)+\frac{i+1}{i+2}\,T_{i+3}^{*}(\rho)\right)\left(\sum_{k=1}^{j}\left(\mathscr{F}_{k,\,j}\,T_k^{*}(t)+\mathscr{G}_j\right)\right),\end{aligned} \tag{44}$$

$$\zeta^M(\rho,t)\,\zeta^M_\rho(\rho,t)=\sum_{p=0}^{M}\sum_{q=0}^{M}\hat{\xi}_{pq}\,\mathscr{X}_p(\rho)\,\mathscr{T}_q(t)\times\sum_{i=0}^{M}\sum_{j=0}^{M}\hat{\xi}_{ij}\left(\sum_{p=0}^{i-1}\mathscr{A}_{p,\,i}\,T^*_p(\rho)\right.$$

$$\left.-\frac{i+1}{i+2}\sum_{p=0}^{i}\mathscr{A}_{p,\,i+1}\,T^*_p(\rho)-\sum_{p=0}^{i+1}\mathscr{A}_{p,\,i+2}\,T^*_p(\rho)+\frac{i+1}{i+2}\sum_{p=0}^{i+2}\mathscr{A}_{p,\,i+3}\,T^*_p(\rho)\right)\mathscr{T}_j(t)$$

$$=t^{2\alpha}\sum_{q=0}^{M}\hat{\xi}_{pq}\left(T^*_i(\rho)-\frac{i+1}{i+2}\,T^*_{i+1}(\rho)-T^*_{i+2}(\rho)+\frac{i+1}{i+2}\,T^*_{i+3}(\rho)\right)T^*_q(t)$$

$$\times\sum_{i=0}^{M}\sum_{j=0}^{M}\hat{\xi}_{ij}\left(\sum_{p=0}^{i-1}\mathscr{A}_{p,\,i}\,T^*_p(\rho)\right.$$

$$\left.-\frac{i+1}{i+2}\sum_{p=0}^{i}\mathscr{A}_{p,\,i+1}\,T^*_p(\rho)-\sum_{p=0}^{i+1}\mathscr{A}_{p,\,i+2}\,T^*_p(\rho)+\frac{i+1}{i+2}\sum_{p=0}^{i+2}\mathscr{A}_{p,\,i+3}\,T^*_p(\rho)\right)T^*_j(t), \tag{45}$$

$$\zeta^M_\rho(\rho,t)=t^{\alpha}\sum_{i=0}^{M}\sum_{j=0}^{M}\hat{\xi}_{ij}\left(\sum_{p=0}^{i-1}\mathscr{A}_{p,\,i}\,T^*_p(\rho)-\frac{i+1}{i+2}\sum_{p=0}^{i}\mathscr{A}_{p,\,i+1}\,T^*_p(\rho)-\sum_{p=0}^{i+1}\mathscr{A}_{p,\,i+2}\,T^*_p(\rho)\right.$$

$$\left.+\frac{i+1}{i+2}\sum_{p=0}^{i+2}\mathscr{A}_{p,\,i+3}\,T^*_p(\rho)\right)T^*_j(t), \tag{46}$$

$$\zeta^M_{\rho\rho}(\rho,t)=t^{\alpha}\sum_{i=0}^{M}\sum_{j=0}^{M}\hat{\xi}_{ij}\left(\sum_{p=0}^{i-2}\mathscr{B}_{p,\,i}\,T^*_p(\rho)-\frac{i+1}{i+2}\sum_{p=0}^{i-1}\mathscr{B}_{p,\,i+1}\,T^*_p(\rho)-\sum_{p=0}^{i}\mathscr{B}_{p,\,i+2}\,T^*_p(\rho)\right.$$

$$\left.+\frac{i+1}{i+2}\sum_{p=0}^{i+1}\mathscr{B}_{p,\,i+3}\,T^*_p(\rho)\right)T^*_j(t), \tag{47}$$

$$\zeta^M_{\rho\rho\rho}(\rho,t)=t^{\alpha}\sum_{i=0}^{M}\sum_{j=0}^{M}\hat{\xi}_{ij}\left(\sum_{p=0}^{i-3}\mathscr{C}_{p,\,i}\,T^*_p(\rho)-\frac{i+1}{i+2}\sum_{p=0}^{i-2}\mathscr{C}_{p,\,i+1}\,T^*_p(\rho)-\sum_{p=0}^{i-1}\mathscr{C}_{p,\,i+2}\,T^*_p(\rho)\right.$$

$$\left.+\frac{i+1}{i+2}\sum_{p=0}^{i}\mathscr{C}_{p,\,i+3}\,T^*_p(\rho)\right)T^*_j(t). \tag{48}$$

Now, inserting equations (44)-(48) into equation (43) to get the residual $\mathbb{RES}(\rho,t)$ in simple form. And hence, the application of collocation method at some collocation points (ρ_i,t_j) enables us to get system of equations resulting from

$$\mathbb{RES}(\rho_i, t_j) = 0, \tag{49}$$

where $\{(\rho_i, t_j) : i, j = 1, 2, ..., M+1\}$ are the first distinct roots of $T^*_{M+1}(\rho)$ and $T^*_{M+1}(t)$.

Solving the resulting $(M+1)^2$ nonlinear system from (49) through Newton's iterative method enables us to get the expansion coefficients $\hat{\zeta}_{ij}$.

4. Illustrative examples

Example 1 Consider the following TFKdVB equation

$$D_t^{\alpha}\varphi(\rho, t) + \varphi(\rho, t)\,\varphi_{\rho}(\rho, t) - \varphi_{\rho\rho}(\rho, t) + \varphi_{\rho\rho\rho}(\rho, t) = s(\rho, t), \quad \alpha \in (0, 1), \tag{50}$$

subject to

$$\begin{aligned} &\varphi(\rho, 0) = 0, \quad \rho \in [0, 1], \\ &\varphi(0, t) = \varphi(1, t) = \varphi_{\rho}(1, t) = 0, \quad t \in [0, 1], \end{aligned} \tag{51}$$

where $\varphi(\rho, t) = t^{\alpha+1}(\rho - 1)^2(e^{\rho} - 1)$ is the exact solution of equations (50) and (51) and $s(\rho, t)$ is determined by equation (50) compatible with the solution chosen.

The absolute errors (AE) obtained via the suggested method are shown in Table 1 when $\alpha = 0.1$ and $M = 12$ indicating that it is effective in providing a highly precise approximation of the exact solution. The AE for various values of M at $\alpha = 0.5$ are shown in Figure 1. This figure verifies that the suggested approach reduces errors consistently throughout the domain and shows a good agreement of the approximate solution with the exact one. The L_{∞} errors at various M values when $\alpha = 0.8$ and $0 < \rho < 1$ are shown in Table 2.

Table 1. The AE of Example 1 at $\alpha = 0.1$, $M = 12$

ρ	$t = 0.2$	$t = 0.4$	$t = 0.6$	$t = 0.8$
0.1	2.25514×10^{-17}	3.1225×10^{-17}	4.85723×10^{-17}	5.55112×10^{-17}
0.2	1.04083×10^{-17}	1.38778×10^{-17}	1.38778×10^{-17}	4.16334×10^{-17}
0.3	2.08167×10^{-17}	5.55112×10^{-17}	2.77556×10^{-17}	5.55112×10^{-17}
0.4	6.93889×10^{-18}	1.38778×10^{-17}	1.38778×10^{-17}	2.77556×10^{-17}
0.5	6.93889×10^{-18}	2.77556×10^{-17}	0	0
0.6	6.93889×10^{-18}	6.93889×10^{-18}	4.16334×10^{-17}	2.77556×10^{-17}
0.7	3.4694×10^{-18}	2.08167×10^{-17}	6.93889×10^{-18}	1.38778×10^{-17}
0.8	1.73472×10^{-18}	6.93889×10^{-18}	3.46945×10^{-18}	1.38778×10^{-17}
0.9	4.33681×10^{-19}	3.46945×10^{-18}	0	3.46945×10^{-18}

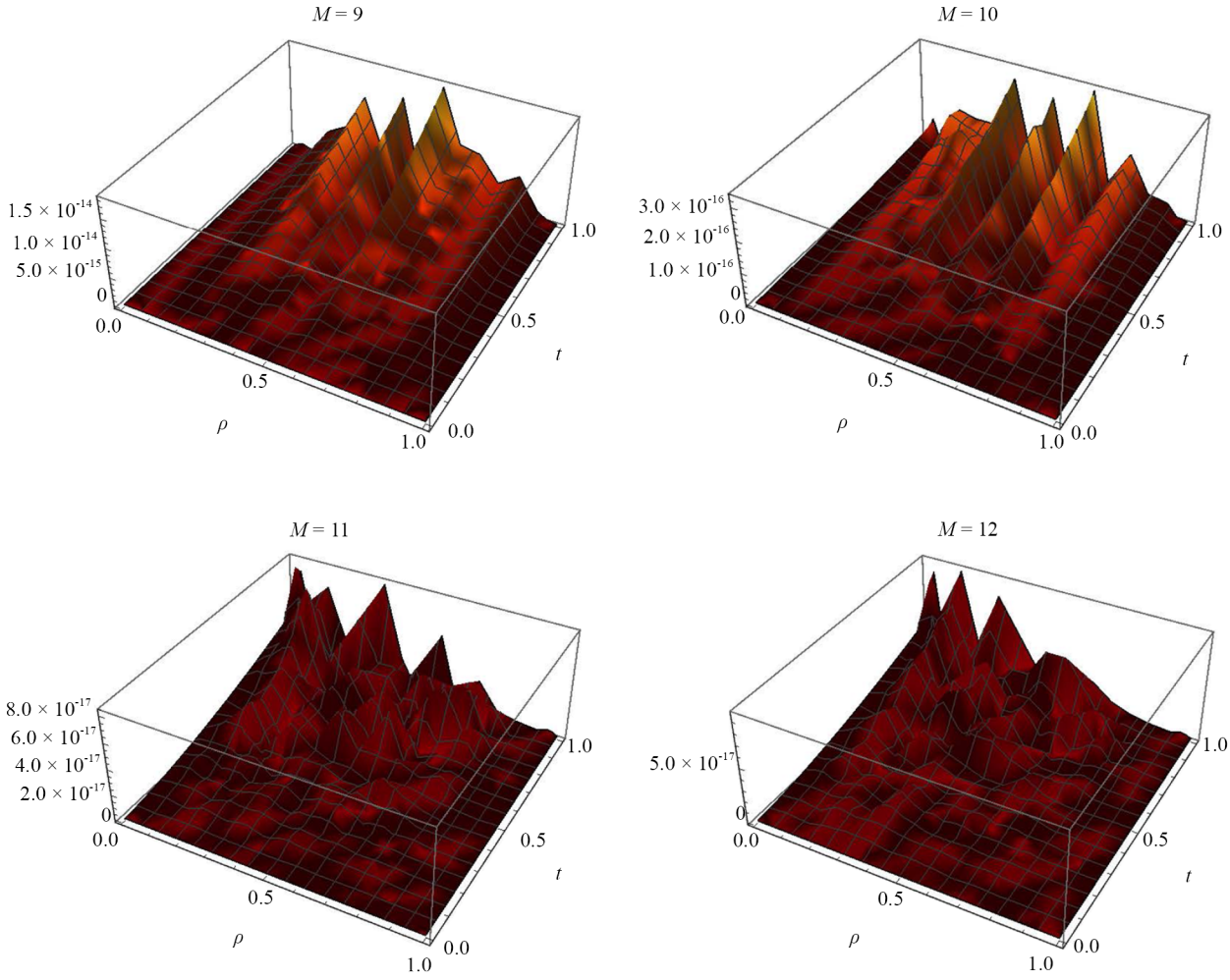

Figure 1. The AE of Example 1 at different values of M when $\alpha = 0.5$

Table 2. The L_∞ errors of Example 1 at $\alpha = 0.8$ when $0 < \rho < 1$

t	$M = 8$	$M = 9$	$M = 10$	$M = 12$
0.1	1.46267×10^{-14}	2.94517×10^{-16}	7.26408×10^{-18}	2.74362×10^{-18}
0.2	5.14033×10^{-14}	1.03025×10^{-15}	2.77012×10^{-17}	1.26571×10^{-17}
0.3	1.07023×10^{-13}	2.14185×10^{-15}	5.10593×10^{-17}	1.63399×10^{-17}
0.4	1.79949×10^{-13}	3.59673×10^{-15}	7.9806×10^{-17}	2.66927×10^{-17}
0.5	2.69253×10^{-13}	5.38878×10^{-15}	1.01587×10^{-16}	4.51448×10^{-17}
0.6	3.74182×10^{-13}	1.081297×10^{-15}	1.81261×10^{-16}	5.5645×10^{-17}
0.7	4.94191×10^{-13}	9.89275×10^{-15}	2.59759×10^{-16}	9.35842×10^{-17}
0.8	6.28811×10^{-13}	1.25506×10^{-14}	2.93204×10^{-16}	8.74225×10^{-17}
0.9	7.77725×10^{-13}	1.55053×10^{-14}	3.76842×10^{-16}	1.28302×10^{-16}

Example 2 [32–34] Consider the following TFKdVB equation

$$D_t^{\alpha}\varphi(\rho,t)+\varphi(\rho,t)\,\varphi_{\rho}(\rho,t)-\varphi_{\rho\rho}(\rho,t)+\varphi_{\rho\rho\rho}(\rho,t)=s(\rho,t),\quad \alpha\in(0,1), \tag{52}$$

subject to

$$\begin{aligned}&\varphi(\rho,0)=0,\quad \rho\in[0,1],\\ &\varphi(0,t)=\varphi(1,t)=\varphi_{\rho}(1,t)=0,\quad t\in[0,1],\end{aligned} \tag{53}$$

where $\varphi(\rho,t)=t^{\alpha}(\rho-1)^4\sin(\pi\rho)$ is the exact solution of equations (52) and (53) and $s(\rho,t)$ is determined by equation (52) consistent with the chosen solution.

A comparison of the L_2 error at $\alpha=0.4$ and $\alpha=0.8$ between present technique and the method in [32] is shown in Table 3. A comparison of the L_∞ at at various values of α between current technique and the method in [33] is shown in Table 4. A comparison of the maximum errors at $\alpha=0.4$ between current technique and the method in [34] is shown in Table 5. We see in these tables that the results are accurate for small choices of M. Also, these comparisons reveal the superior performance of our technique over methods in [32–34]. When $\alpha=0.9$ and $t=0.5$, the AE is displayed for various M values in Figure 2. The approximate and exact solutions at $\alpha=0.4$ and $M=16$ is shown in Figure 3. When $\alpha=0.5$, the AE is shown at various M values in Figure 4. Lastly, for $M=16$ and $0<\rho<1$, Table 6 displays the L_∞ errors at various values of t.

Table 3. Comparison of L_2 errors of Example 2

α	0.4	0.8
Method in [32] at $M=\lceil N^{\min\{r\alpha,2\}}\rceil,\ r=3,\ N=32$	9.8238×10^{-3}	6.4395×10^{-4}
Method in [32] at $N=100,\ r=\dfrac{2}{\alpha},\ M=16$	4.7068×10^{-4}	4.5241×10^{-4}
Our method at $M=16$	7.45931×10^{-17}	5.9848×10^{-17}

Table 4. Comparison of L_∞ errors of Example 2

α	0.25	0.5	0.75
Method in [33] at $\Delta t=0.0025,\ \Delta x=0.00125$	1.20402×10^{-5}	1.99941×10^{-5}	1.63596×10^{-5}
Our method at $M=16$	1.38778×10^{-16}	7.11237×10^{-17}	4.74881×10^{-17}

Table 5. Comparison of maximum errors of Example 2 at $\alpha=0.4$

t	Method in [34] at $M=100$	Our method at $M=16$
0.25	2.1265×10^{-7}	6.93889×10^{-17}
0.125	1.2387×10^{-8}	8.32667×10^{-17}
0.0625	3.9521×10^{-9}	5.55112×10^{-17}

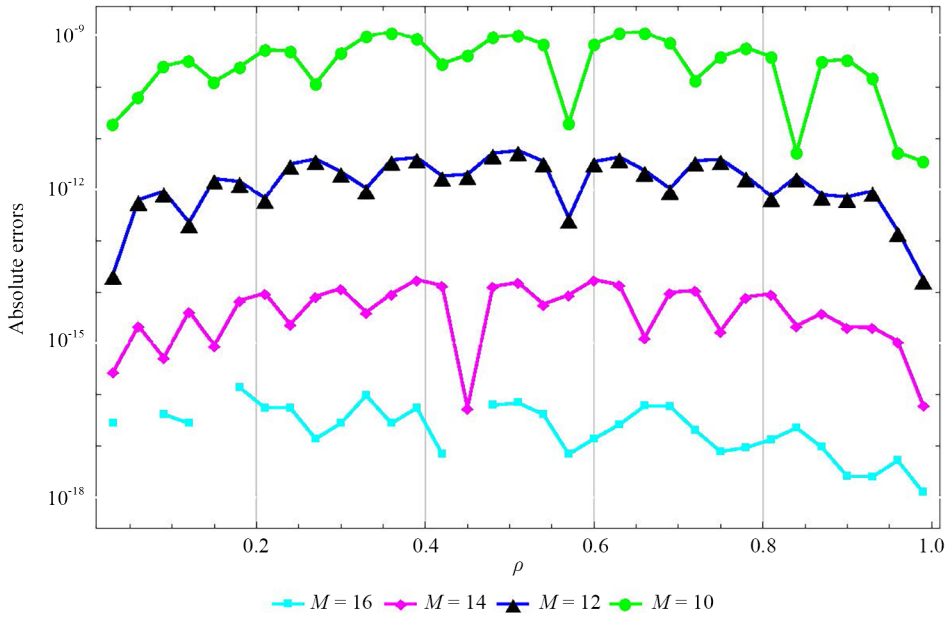

Figure 2. The AE for Example 2 at different values of M for $\alpha = 0.9$ and $t = 0.5$

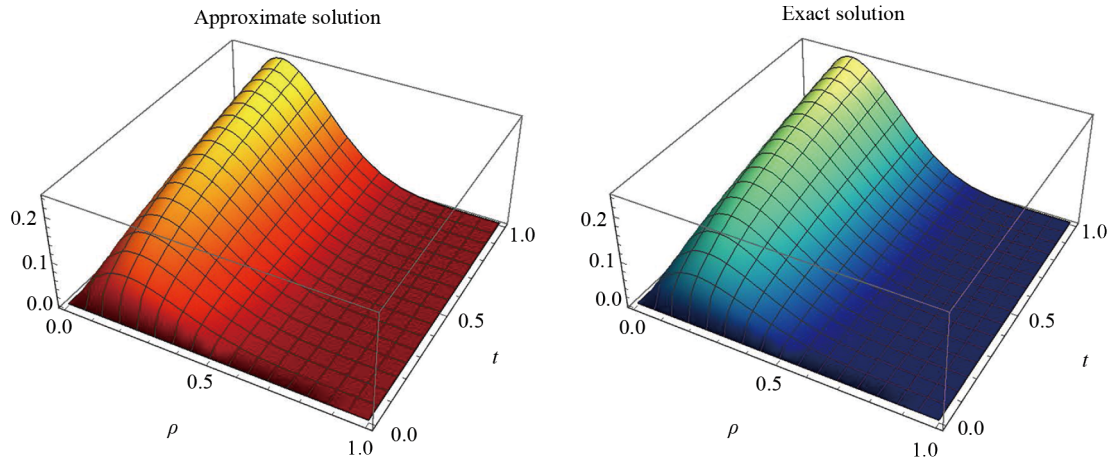

Figure 3. The approximate and exact solutions for Example 2 at $\alpha = 0.4$ and $M = 16$

Table 6. The L_∞ errors of Example 2 at $M = 16$ when $0 < \rho < 1$

α	$t = 0.1$	$t = 0.3$	$t = 0.5$	$t = 0.7$	$t = 0.9$
0.4	8.32667×10^{-17}	1.249×10^{-16}	1.66533×10^{-16}	2.77556×10^{-16}	1.94289×10^{-16}
0.8	4.16334×10^{-17}	9.71445×10^{-17}	1.38778×10^{-16}	1.66533×10^{-16}	1.66533×10^{-16}
0.9	3.1225×10^{-17}	8.32667×10^{-17}	9.71445×10^{-17}	2.498×10^{-16}	2.77556×10^{-16}

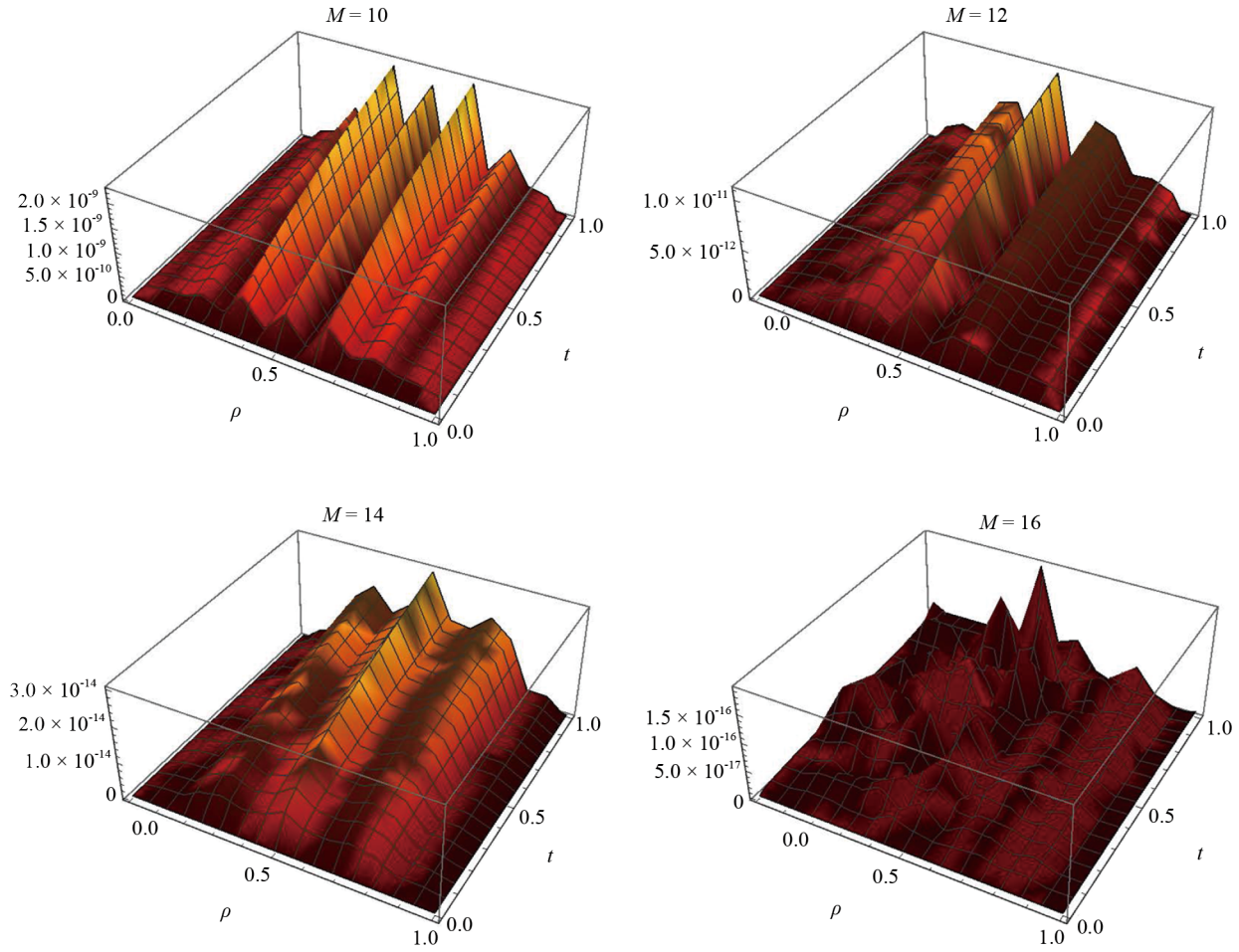

Figure 4. The AE of Example 2 at different values of M when $\alpha = 0.5$

Example 3 Consider the following TFKdVB equation

$$D_t^{\alpha}\varphi(\rho,t)+\varphi(\rho,t)u_{\rho}(\rho,t)-\varphi_{\rho\rho}(\rho,t)+\varphi_{\rho\rho\rho}(\rho,t)=s(\rho,t),\quad \alpha\in(0,1), \tag{54}$$

subject to

$$\begin{aligned}&\varphi(\rho,0)=0,\quad \rho\in[0,1],\\ &\varphi(0,t)=\varphi(1,t)=\varphi_{\rho}(1,t)=0,\quad t\in[0,1],\end{aligned} \tag{55}$$

where $\varphi(\rho,t)=t^{\alpha}\rho^{6}(\rho-1)^{2}$ is the exact solution of equations (54) and (55) and $s(\rho,t)$ is determined by equation (54) consistent with the chosen solution.

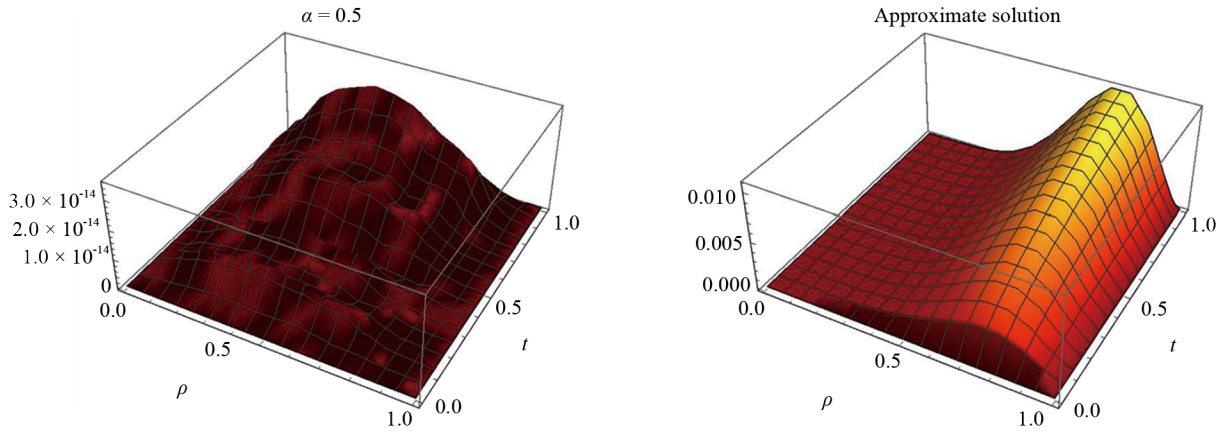

Figure 5. The AE (left) at $\alpha = 0.5$ and approximate solution (right) for Example 3 when $M = 8$

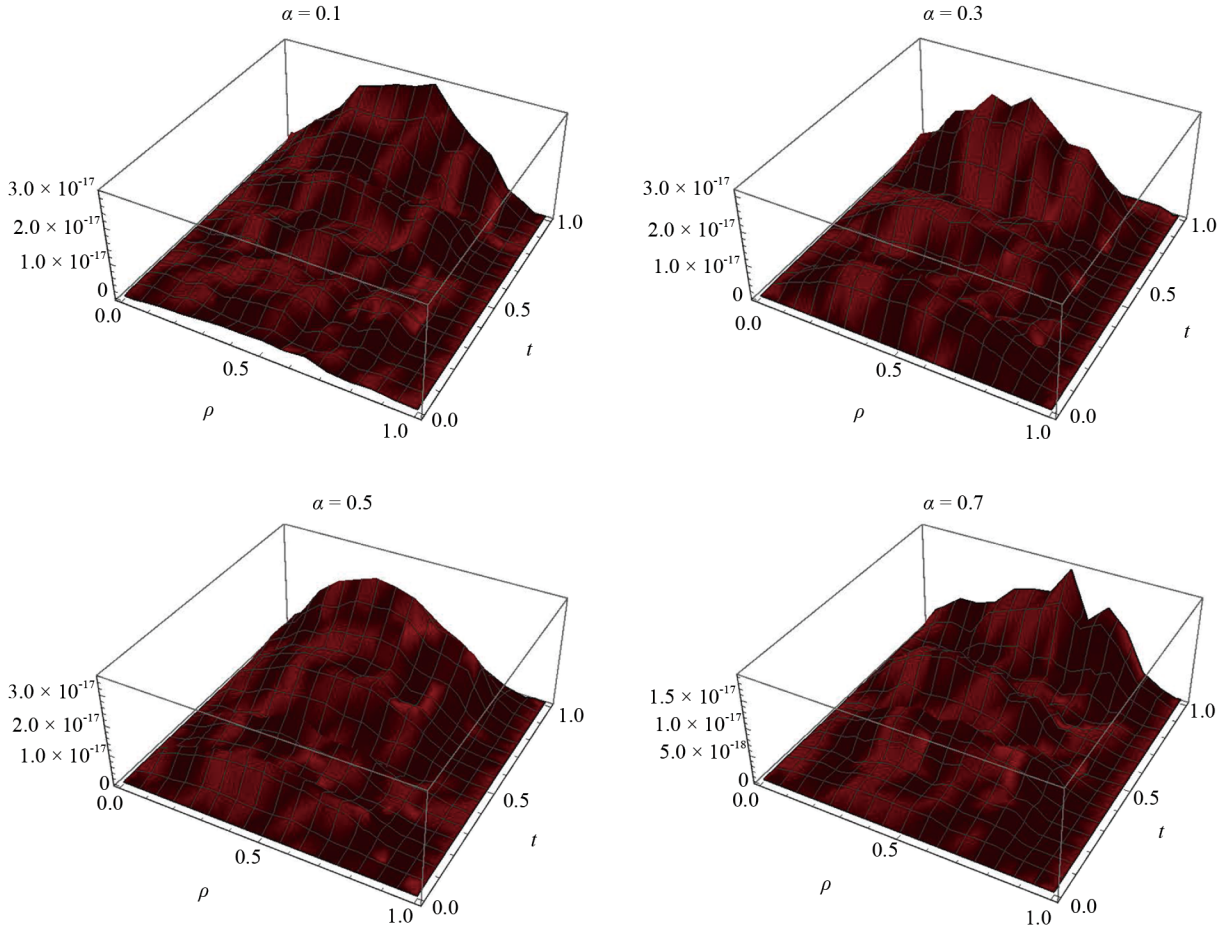

Figure 6. The AE at different values of α for Example 3 when $M = 8$

When $M = 8$ and $0 < \rho < 1$, the L_∞ errors at various values of t are shown in Table 7. The AE (left) and approximate solution (right) for $\alpha = 0.5$ when $M = 8$ are shown in Figure 5. This figure verifies that the suggested approach reduces errors consistently throughout the domain and shows a good agreement of the approximate solution with the exact one.

Finally, AE at different values of α when $M = 8$ is shown in Figure 6. These results show a good agreement of the approximate solution with the exact one.

Table 7. The L_∞ errors of Example 3 at $M = 8$ when $0 < \rho < 1$

t	$\alpha = 0.1$	$\alpha = 0.3$	$\alpha = 0.7$	$\alpha = 0.9$
0.1	8.84135×10^{-18}	1.57973×10^{-17}	3.50205×10^{-18}	2.0818×10^{-18}
0.2	1.40214×10^{-17}	6.98989×10^{-18}	2.83771×10^{-18}	2.23368×10^{-18}
0.3	1.10246×10^{-17}	6.56947×10^{-18}	8.54358×10^{-18}	4.17422×10^{-18}
0.4	9.03536×10^{-18}	1.09822×10^{-17}	7.76784×10^{-18}	6.16994×10^{-18}
0.5	1.03383×10^{-17}	1.52032×10^{-17}	8.88143×10^{-18}	1.00522×10^{-17}
0.6	1.34581×10^{-17}	1.08129×10^{-17}	1.47084×10^{-17}	1.5391×10^{-17}
0.7	1.48034×10^{-17}	1.18643×10^{-17}	6.18619×10^{-18}	1.703×10^{-17}
0.8	1.43422×10^{-17}	2.79832×10^{-17}	1.23383×10^{-17}	9.69681×10^{-18}
0.9	1.18495×10^{-17}	1.70481×10^{-17}	1.09176×10^{-17}	1.07276×10^{-17}

5. Concluding remarks

We created a numerical method using the collocation technique to solve the TFKdVB problem. Shifted Chebyshev polynomials may effectively handle fractional derivatives in both space and temporal dimensions. The scheme for solving fractional partial differential equations is efficient and accurate, as demonstrated by numerical experiments. Further research could apply this approach to more complex equations with higher-order derivatives or non-linear terms. This method could be extended to more complicated equations with non-linear components or higher-order derivatives in future studies. Investigating linked systems of time-fractional equations, where the interplay of several equations presents extra difficulties, is a possible extension of this work. To further investigate the method's resilience and adaptability, it might be modified for three-dimensional situations or equations with stochastic terms. Lastly, hybrid approaches that integrate machine learning techniques with this collocation methodology may present interesting paths toward increasing accuracy and speeding up calculations in large-scale applications.

Conflict of interest

The authors declare no competing financial interest.

References

[1] Korteweg DJ, De Vries G. On the change of form of long waves advancing in a rectangular channel, and a new type of long stationary wave. *Philosophical Magazine*. 1895; 39: 422-443.

[2] Su CH, Gardner CS. Korteweg-de Vries equation and generalizations III. Derivation of the Korteweg-de Vries equation and Burgers equation. *Journal of Mathematical Physics*. 1969; 10(3): 536-539. Available from: https://doi.org/10.1063/1.1664873.

[3] Wang Q. Homotopy perturbation method for fractional KdV-Burgers equation. *Chaos, Solitons & Fractals*. 2008; 35(5): 843-850. Available from: https://doi.org/10.1016/j.chaos.2006.05.074.

[4] Golmankhaneh AK, Baleanu D. Homotopy perturbation method for solving a system of Schrödinger-Korteweg-de Vries equations. *Romanian Reports in Physics*. 2011; 63(3): 609-623.

[5] Bhrawy AH, Zaky MA, Baleanu D. New numerical approximations for space-time fractional Burgers' equations via a Legendre spectral-collocation method. *Romanian Reports in Physics*. 2015; 67: 340-349.

[6] Atta AG, Abd-Elhameed WM, Moatimid GM, Youssri YH. Novel spectral schemes to fractional problems with nonsmooth solutions. *Mathematical Methods in the Applied Sciences*. 2023; 46(13): 14745-14764. Available from: https://doi.org/10.1002/mma.9343.

[7] Bose CSV, Udhayakumar R, Muthukumaran V, Al-Omari S. A study on approximate controllability of Ψ-Caputo fractional differential equations with impulsive effects. *Contemporary Mathematics*. 2024; 5(1): 175-198. Available from: https://doi.org/10.37256/cm.5120243539.

[8] Bose CSV, Udhayakumar R. Approximate controllability of Ψ-Caputo fractional differential equation. *Mathematical Methods in the Applied Sciences*. 2023; 46(17): 17660-17671. Available from: https://doi.org/10.1002/mma.9523.

[9] Atta AG, Youssri YH. Shifted second-kind Chebyshev spectral collocation-based technique for time-fractional KdV-Burgers' equation. *Iranian Journal of Mathematical Chemistry*. 2023; 14(4): 207-224. Available from: https://doi.org/10.22052/ijmc.2023.252824.1710.

[10] Inc M, Parto-Haghighi M, Akinlar MA, Chu YM. New numerical solutions of fractional-order Korteweg-de Vries equation. *Results in Physics*. 2020; 19: 103326. Available from: https://doi.org/10.1016/j.rinp.2020.103326.

[11] Shi Y, Xu B, Guo Y. Numerical solution of Korteweg-de Vries-Burgers equation by the compact-type CIP method. *Advances in Difference Equations*. 2015; 2015: 1-9. Available from: https://doi.org/10.1186/s13662-015-0682-5.

[12] Yousif MA, Guirao JL, Mohammed PO, Chorfi N, Baleanu D. A computational study of time-fractional gas dynamics models by means of conformable finite difference method. *AIMS Mathematics*. 2024; 9(7): 19843-19858. Available from: https://doi.org/10.3934/math.2024969.

[13] Yousif MA, Hamasalh FK. Conformable non-polynomial spline method: A robust and accurate numerical technique. *Ain Shams Engineering Journal*. 2024; 15(2): 102415. Available from: https://doi.org/10.1016/j.asej.2023.102415.

[14] Mohammed PO, Agarwal RP, Brevik I, Abdelwahed M, Kashuri A, Yousif MA. On multiple-type wave solutions for the nonlinear coupled time-fractional Schrödinger model. *Symmetry*. 2024; 16(5): 553. Available from: https://doi.org/10.3390/sym16050553.

[15] Abd-Elhameed WM, Youssri HY, Atta AG. Tau algorithm for fractional delay differential equations utilizing seventh-kind Chebyshev polynomials. *Journal of Mathematical Modeling*. 2024; 12(2): 277-299. Available from: https://doi.org/10.22124/jmm.2024.25844.2295.

[16] Youssri HY, Atta AG. Modal spectral Tchebyshev Petrov-Galerkin stratagem for the time-fractional nonlinear Burgers' equation. *Iranian Journal of Numerical Analysis and Optimization*. 2024; 14(1): 172-199. Available from: https://doi.org/10.22067/ijnao.2023.83389.1292.

[17] Youssri YH, Ismail MI, Atta AG. Chebyshev Petrov-Galerkin procedure for the time-fractional heat equation with nonlocal conditions. *Physica Scripta*. 2023; 99(1): 015251. Available from: https://doi.org/10.1088/1402-4896/ad1700.

[18] Youssri YH, Atta AG, Moustafa MO, Abu Waar ZY. Explicit collocation algorithm for the nonlinear fractional Duffing equation via third-kind Chebyshev polynomials. *Iranian Journal of Numerical Analysis and Optimization*. 2025; 2025: 1543. Available from: https://doi.org/10.22067/ijnao.2025.90483.1543.

[19] Hughes TJR. *The Finite Element Method: Linear Static and Dynamic Finite Element Analysis*. New York: Dover Publications; 2012.

[20] Boyd JP. *Spectral Methods for Partial Differential Equations*. Philadelphia, Pennsylvania, United States: SIAM; 2001.

[21] Atta AG, Soliman JF, Elsaeed EW, Elsaeed MW, Youssri YH. Spectral collocation algorithm for the fractional Bratu equation via hexic shifted Chebyshev polynomials. *Computational Methods for Differential Equations*. 2024; 2024: 2621. Available from: https://doi.org/10.22034/cmde.2024.61045.2621.

[22] Atta AG, Abd-Elhameed WM, Youssri YH. Approximate collocation solution for the time-fractional Newell-Whitehead-Segel equation. *Journal of Applied and Computational Mechanics*. 2024; 2024: 4686. Available from: https://doi.org/10.22055/jacm.2024.47269.4686.

[23] Abd-Elhameed WM, Ahmed HM, Zaky MA, Hafez RM. A new shifted generalized Chebyshev approach for multi-dimensional sinh-Gordon equation. *Physica Scripta*. 2024; 99(9): 095269. Available from: https://dx.doi.org/10.1088/1402-4896/ad6fe3.

[24] Ahmed HM, Abd-Elhameed WM. Spectral solutions of specific singular differential equations using a unified spectral Galerkin-collocation algorithm. *Journal of Nonlinear Mathematical Physics*. 2024; 31(1): 42. Available from: https://doi.org/10.1007/s44198-024-00194-0.

[25] Ahmed HM, Hafez RM, Abd-Elhameed WM. A computational strategy for nonlinear time-fractional generalized Kawahara equation using new eighth-kind Chebyshev operational matrices. *Physica Scripta*. 2024; 99(4): 045250. Available from: https://dx.doi.org/10.1088/1402-4896/ad3482.

[26] Abd-Elhameed WM, Ahmed HM. Spectral solutions for the time-fractional heat differential equation through a novel unified sequence of Chebyshev polynomials. *AIMS Mathematics*. 2024; 9(1): 2137-2166. Available from: https://doi.org/10.3934/math.2024107.

[27] Abdelghany EM, Abd-Elhameed WM, Moatimid GM, Youssri HY, Atta AG. A Tau approach for solving time-fractional heat equation based on the shifted sixth-kind Chebyshev polynomials. *Symmetry*. 2023; 15(3): 594. Available from: https://doi.org/10.3390/sym15030594.

[28] Podlubny I. *Fractional Differential Equations*. PA, USA: Elsevier; 1998.

[29] Youssri YH, Atta AG. Double TChebyshev spectral tau algorithm for solving KdV equation, with soliton application. In: *Solitons*. New York, NY: Springer; 2022. p.451-467. Available from: https://doi.org/10.1007/978-1-0716-2457-9_771.

[30] Abd-Elhameed WM, Machado JAT, Youssri YH. Hypergeometric fractional derivatives formula of shifted Chebyshev polynomials: tau algorithm for a type of fractional delay differential equations. *International Journal of Nonlinear Sciences and Numerical Simulation*. 2022; 23(7-8): 1253-1268. Available from: https://doi.org/10.1515/ijnsns-2020-0124.

[31] Askey R. *Orthogonal Polynomials and Special Functions*. PA, USA: SIAM; 1975.

[32] Cen D, Wang Z, Mo Y. Second order difference schemes for time-fractional KdV-Burgers' equation with initial singularity. *Applied Mathematics Letters*. 2021; 112: 106829. Available from: https://doi.org/10.1016/j.aml.2020.106829.

[33] Karaagac B, Esen A, Owolabi KM, Pindza E. A collocation method for solving time fractional nonlinear Korteweg-de Vries-Burgers equation arising in shallow water waves. *International Journal of Modern Physics C*. 2023; 34(7): 2350096. Available from: https://doi.org/10.1142/S0129183123500961.

[34] Vivas-Cortez M, Yousif MA, Mahmood BA, Mohammed PO, Chorfi N, Lupas AA. High-accuracy solutions to the time-fractional KdV-Burgers equation using rational non-polynomial splines. *Symmetry*. 2024; 17(1): 16. Available from: https://doi.org/10.3390/sym17010016.